JOURNAL OF PROPULSION AND POWER
Vol. 12, No. 2, March–April 1996

Active Cooling of Metal Oxide Semiconductor Controlled Thyristor Using Venturi Flow

R. Ponnappan*
UES, Inc., Dayton, Ohio 45432
and
J. E. Leland,† W. S. Chang,† J. E. Beam,‡ B. T. Nguyen,§ and J. A. Weimer¶
U.S. Air Force Wright Laboratory, Wright–Patterson Air Force Base, Ohio 45433

A metal oxide semiconductor controlled thyristor (MCT) is a solid-state high-current switching device. Because of its high-current and high-heat dissipation, this device requires an advanced cooling arrangement. A sample MCT device was successfully tested in a conduction mode up to 95 A using a new technique called venturi cooling. Steady-state operational tests were performed under various coolant temperatures and flow rates. The highest device temperature was 168.5°C, whereas the power dissipation and heat flux were 170 W and 257 W/cm², respectively. Comparison with a commercial liquid-cooled cold plate showed that the cooling effectiveness is nearly double for the venturi flow. Measured junction-to-case thermal resistance of the MCT was 0.213°C/W for venturi flow compared to 0.421°C/W for the commercial cold plate. Venturi flow cooling is highly recommended for MCT applications.

Nomenclature

A	=	area, cm²
l_t	=	throat length and heat addition length, m
Nu	=	Nusselt number
P	=	power dissipation, W
Pr	=	Prandtl number
q_1, q_2	=	heat flux, W/cm²
Re	=	upstream flow Reynolds number
T	=	temperature, °C
T_w	=	fluid side wall temperature, °C
ΔT	=	temperature difference, °C
θ_{DF}	=	thermal resistance (device-to-fluid), °C/W
θ_{JC}	=	thermal resistance (junction-to-case), °C/W

Subscripts

Base	=	base surface area of the MCT device
Bottom	=	bottom face of the MCT
Fluid	=	coolant
MCT	=	MCT device
Substrate	=	substrate area of the silicon die in MCT
Top	=	top face of the MCT

Introduction

THE new solid-state switching device called metal oxide semiconductor (MOS) controlled thyristor (MCT) can handle high currents at reasonably fast switching speeds.[1] This high-power switching device, a key component in the power inverter design, is critical to the success of the integrated starter/generator, integrated power unit, high reliability generator, and solid-state power controller programs. The MCT is the newest semiconductor switch technology and promises the lowest switch-forward voltage-drop and inverter losses.[2]

The MCT operates at current densities of 150–200 A/cm² over an active die area of <1 cm², resulting in a heat flux of over 400 W/cm². Although generally operated in a low-duty cycle-pulsed mode for inverters and motor controllers, the steady-state heat levels for these devices will be limited to about 100 W/cm². If operated in a continuous mode as a power control switch, a single MCT could generate a continuous heat load of 200 W or more with the junction temperature restricted not to exceed 150°C.[3] This has drawn the attention of heat transfer engineers for investigating suitable and effective cooling techniques.

For direct immersion cooling or flow-through two-phase cooling, fluorocarbon (FC) fluids are widely considered by the electronic industry. Recent research results from the literature show that the highest heat flux (≈critical heat flux) obtained in flow through boiling in a curved channel using FC-72 is 141 W/cm² at T_w = 92°C for a direct contact simulated heat source and 63 W/cm² at T_w = 150°C for an indirect contact MCT device.[4,5] Wadsworth and Mudawar[6] reported a single-phase FC-72 fluid jet impingement cooling heat flux of 80 W/cm² for a smooth surface with a jet velocity of 12.9 m/s and a subcooling of 40°C. A critical heat flux (CHF) value as high as 411 W/cm² was achieved by using a microgroove surface enhancement.[6] Even though the FC fluids have very good dielectric and thermophysical properties, they suffer the disadvantages such as high cost, volatility, and being prone to moisture and air absorption. For typical applications, inexpensive fluids that are easily available are sought. Spray and jet impingement cooling are effective, but relatively difficult to use. Also, the thermal instabilities associated with the spray and two-phase cooling techniques may discourage electronic packaging designers.

A simple, new approach called venturi flow cooling concept was introduced in 1991 and some preliminary results were presented by the authors.[7,8] Various aspects relating to this research such as the choice of fluids, geometry, and flow pressure drop penalty were discussed. Prandtl number range of the fluids [FC-72, water, turbine oil, and poly-alpha olefin (PAO)] at 25°C was 3–227. Annular, pipe, and venturi flow geometries were compared. Under the same flow conditions, venturi flow caused only 37 kPa more pressure drop than pipe

Received Sept. 12, 1994; revision received March 24, 1995; accepted for publication May 8, 1995.

*Principal Research Scientist, Materials and Processes Division. Senior Member AIAA.
†Research Scientist, Aerospace Power Division. Member AIAA.
‡Deputy for Technology, Aerospace Power Division. Associate Fellow AIAA.
§Research Scientist, Aerospace Power Division.
¶Section Chief, Aerospace Power Division.

flow for the given test section. Detailed discussions and results can be found in Refs. 9 and 10. Verification of the test results with heat transfer correlations can be found in Ref. 10.

The scope of the present research was to perform experiments with MCT as integrated in the venturi flow setup using water at various flow rates and temperatures. Water was chosen for convenience and ease of handling. In actual aircraft applications where freezing may become a problem, other fluids discussed earlier could be used. The MCT device was directly mounted on the copper test section to make perfect contact both electrically and thermally. The electrical tests were limited to only the conduction mode with the primary goal of achieving the highest operating current at the lowest possible temperature and thermal resistance. A secondary goal was set to compare the heat transfer enhancements of the venturi cooling with those of the circular pipe flow and commercial liquid-cooled cold plate.

Description of MCT

The MCT technology was still evolving and various packaging configurations existed at the time of this research. The device used in the present study was rated 100 A at 1.554 Vdc and was a five-leaded JEDEC MO-93 plastic package that was a variation of the TO-218 package. This consisted of a silicon die soldered with 0.076 mm of solder to 0.40 mm of copper and encapsulated in 3.56 mm of plastic using silicon alumina metalization. The hermetic package contained a copper–molicopper base with an alumina (ceramic)–copper lid. Additional details and description can be found in Refs. 1 and 11.

Venturi Flow Cooling Concept

Flow through a straight circular tube is converted into a tapering annular flow by positioning a specially shaped bicone constrictor in the center of the tube directly in the flow path. High-power dissipating devices are mounted on the flattened faces directly outside the tube at the throat section. Flow velocity at the throat can be increased beyond an order of magnitude over the upstream velocity. Consequently, Re and Nu are increased for a given high Pr fluid ($5 < Pr < 100$). Boiling of the fluid locally at the throat could affect heat transfer, depending on the wall temperature and fluid properties. The idea of creating high flow velocity is the key to the success of this method. In addition, the effect is very localized to suit the localized heat source such as the MCT device. Device mounting can be in direct or indirect contact with the fluid. By suitable design of the taper angles, the liquid pressure drop due to the venturi can be minimized. Viscosity is a major deciding factor in using this type of convective cooling because the pump power and viscous dissipation effects could outweigh the heat transfer enhancement. It has been shown in this context, by experimental and theoretical investigations, that the pump power penalty is only marginal and that the benefit outweighs the problem.[9]

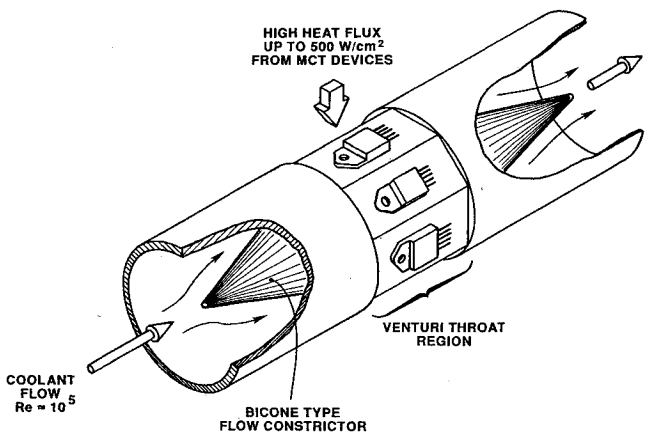

Fig. 1 Annular venturi flow heat sink configuration I.

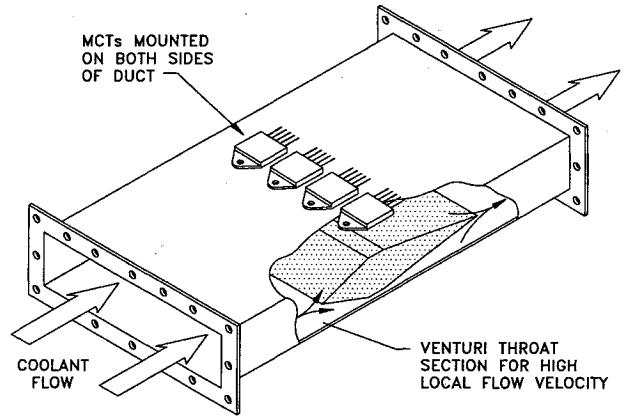

Fig. 2 Rectangular duct flow heat sink configuration II.

MCT Heat Sink–Conceptual Ideas

In actual applications, clusters of MCTs will have to be mounted as a module to share a common heat sink. Two possible heat sink configurations involving venturi concept are illustrated here. Figure 1 shows the cylindrical geometry with planar external mounting surfaces. Figure 2 shows a rectangular duct configuration where both top and bottom panels can be used as heat sinks. Both geometries offer axisymmetrical flow with multistage addition possibilities along the flow direction. The construction material must be aluminum or copper for good wall thermal conductivity. Optimized designs of these conceptual ideas can be worked out if MCT module design and heat loads are known.

Experimental Work

Setup Design

The present experimental setup consisted of a circular copper pipe test section with gasket-seated end flanges for easy removal from and assembly to the coolant flow line. A venturi bicone-flow-constrictor made of stainless steel was rigidly held concentrically inside the test section in order to create the high velocity at the throat section. One of the flat machined faces, located directly outside the throat section, was used for mounting the MCT device. The wall thickness under the MCT varied from 1.58 to 4.34 mm in the circumferential direction because of the hexagonal external geometry. The bicone could be easily removed in order to convert the test section into a circular pipe flow geometry without altering other arrangements.

A schematic diagram of the setup consisting of a constant temperature bath, centrifugal pump, flow meters, filter, pressure transducers, data logger, and a heater circuit is shown in Fig. 3. The heater circuit seen in the figure was replaced with the MCT test circuit. The conduction mode test circuit for the MCT was a relatively simple one consisting of a high-current, low-voltage regulated power supply and a 0.5 mΩ precision shunt resistor for current measurement. The circuit details are shown in Fig. 4. The coolant circulation capacity was 0–35 l/min at temperatures from 5 to 30°C through 3.33-cm-i.d. copper pipe. To compare the relative heat transfer performances, three heat sink geometries were tested. Two were based on the venturi test section and the third was a commercially available liquid-cooled aluminum cold plate. The physical dimensions and details are as follows:

Heat Sink Configuration I

Venturi flow: 1) bicone flow constrictor installed; 2) hydraulic diameter of annular flow = 0.0965 cm; 3) cone angles, upstream = 40 deg and downstream = 20 deg; 4) upstream

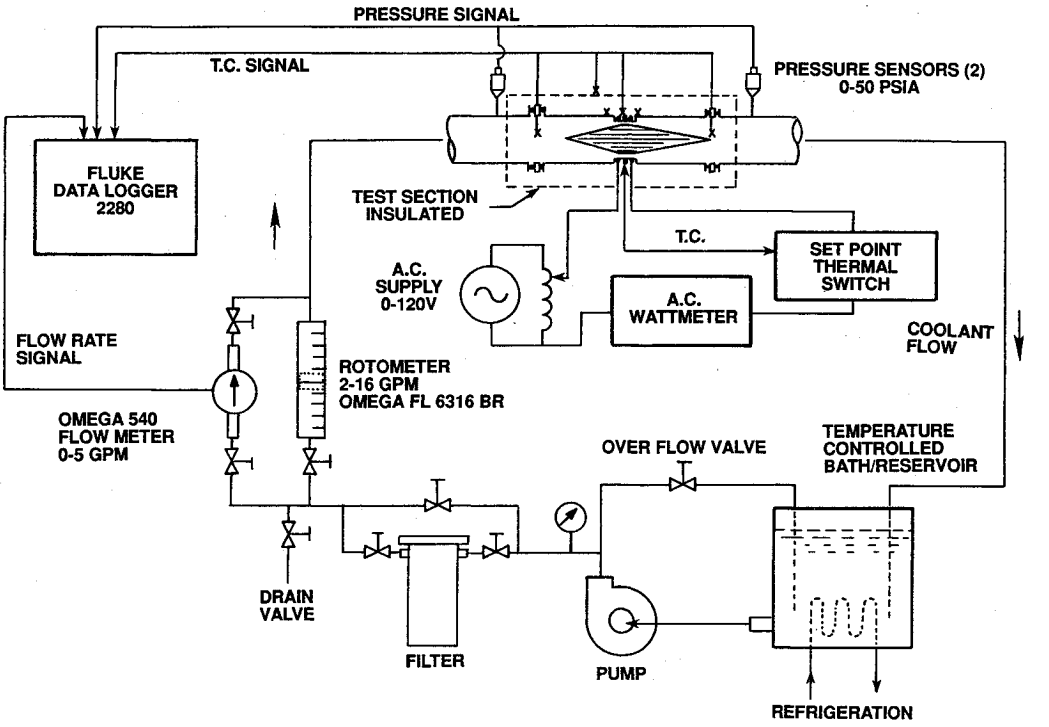

Fig. 3 Experimental test setup schematic diagram.

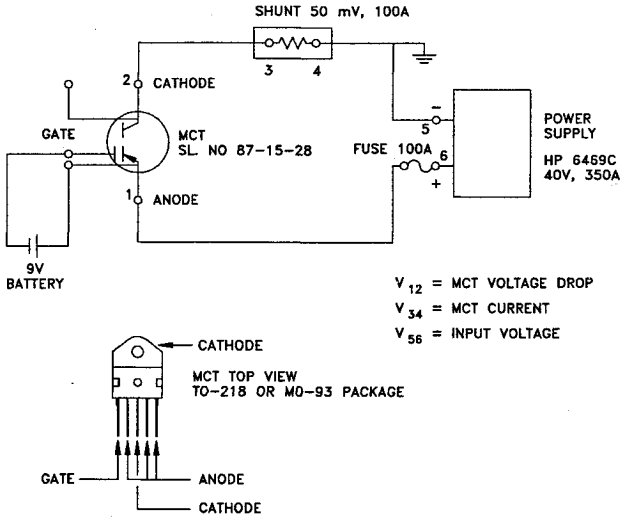

Fig. 4 MCT test circuit (conduction mode).

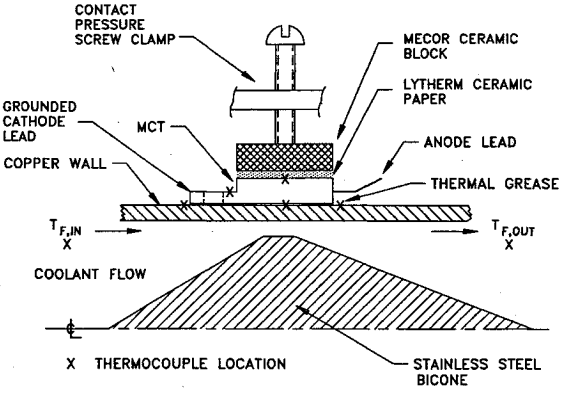

Fig. 5 MCT mounting and thermocouple locations (configurations I and II).

flow diameter = 3.33 cm; 5) venturi section length = 10.5 cm; 6) MCT mounted on one of the six flat faces and clamped by a ring clamp; and 7) because of axisymmetry, a one-sixth share of total flow was assumed to be shared by each face.

Heat Sink Configuration II

Circular-pipe flow: 1) same as configuration I except that the bicone flow constrictor was removed and 2) hydraulic diameter = 3.33 cm.

Heat Sink Configuration III

Commercial cold plate: 1) series 180-10 heat sink by EG&G Wakefield Engineering (1988)[12]; 2) aluminum alloy 6063-T5 plate lined with U-shaped copper tube (9.5 mm o.d., 0.79-mm wall) 30.48 cm long; 3) MCT mounted at the center of plate directly above the inlet side of the copper tubing; and 4) MCT clamped with a special clamp.

MCT and Thermocouple Mounting

The polished metallic surface of the MCT (1.8 cm^2) was mounted on the polished flat surface of the test section with a thin layer of conductive grease applied to both mating surfaces. The top surface of the MCT was pressed down using a ceramic spacer and a 6-mm-diam clamp-screw. A torque of 0.14 N-m was applied using a torque-screw driver that provided consistent contact pressure for the MCT in all of the test configurations.

Thin foil-type thermocouples were used on the top and bottom surfaces of the MCT for temperature sensing. This facilitated the flush-mounting of the MCT. In addition, three other welded-bead-junction thermocouples were mounted on or near the MCT to measure the flange, upstream, and downstream wall temperatures. Inlet and outlet coolant temperatures were measured with probe-type sensors located on the end flanges of the test section.

A grounded-type cathode connection for the MCT facilitated the test section to be at ground potential, even though it was part of the live circuit. Figure 5 illustrates the MCT and thermocouple mounting for test configurations I and II.

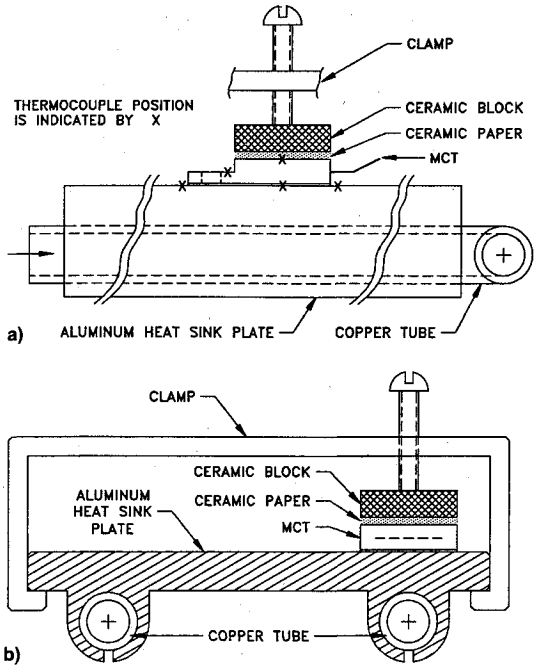

Fig. 6 Commercial liquid-cooled cold plate heat sink configuration III: a) front and b) end views.

Figure 6 shows the views of the commercial heat sink (configuration III).

Test Procedure

Water circulation rate and temperature were set at the desired values. The MCT gate was triggered open by a 9-V battery connected as shown in Fig. 4 and the input power to the circuit was raised by increasing the current from zero to a maximum value in steps of 10 A. Steady-state values of temperatures, voltages, and current were recorded. It took approximately 20 min for each setting. A limiting device temperature of 175°C, measured at the top surface of MCT, was imposed to avoid burning the device. The contact pressure of the MCT was maintained by periodically checking the tightening torque (0.14 N-m) on the clamp–screw. Tests were repeated for coolant temperatures of 6.5, 10, 19.5, and 23°C and varying the flow rate from 0.63 to 6.31 l/min at each coolant temperature. The data were recorded in the Fluke data-logger diskette for further analysis and processing. In a similar manner, tests were repeated for heat sink configuration II and III after suitably modifying the test section.

The temperature measurement accuracy was within ±0.5°C in the range 0–200°C. Electrical power measurement accuracy was within ±1%. Coolant flow was measured using a turbine-type flow meter with ±1% accuracy in the range 0–30 l/min.

Results and Discussion

Temperature Variation

The temperature measurement on the MCT included the top surface, bottom surface, and the flange. The device junction temperature could not be measured with this hermetically sealed package. However, the top surface temperature was assumed to be the junction temperature as the top surface was insulated and the temperature drop between the junction and the top surface was neglected. Even though this caused some inaccuracies, thermal resistances could be calculated and compared for various flow configurations.

Figure 7 shows the MCT top, bottom, and flange, and the wall upstream and downstream temperature variations with MCT power for venturi flow with coolant at 2.52 l/min and 6.5°C. The top surface temperature was the highest and all

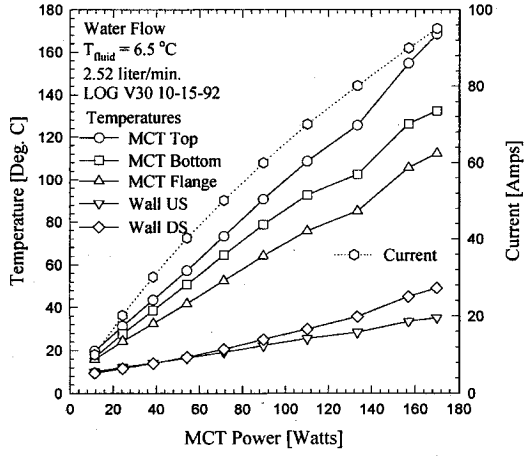

Fig. 7 MCT temperature profile for different MCT power levels.

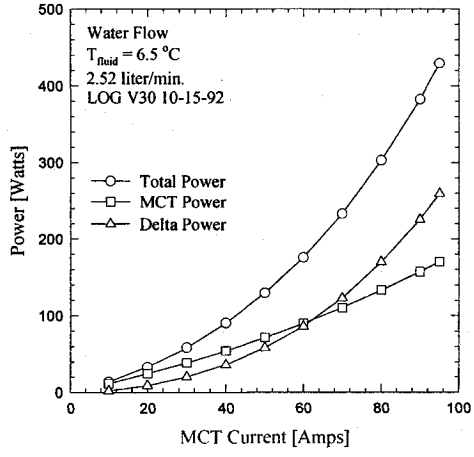

Fig. 8 MCT power vs MCT current.

of the temperature variations were linear with power increase. Figure 8 shows the MCT power variation with MCT current for the same test run as that of Fig. 7. Similar temperature and power variations were observed for circular-pipe flow and commercial heat sink also.

Wall Heat Spreading

Because of the finite wall thickness and high conductivity of the wall material, the heat spreads in the wall to a wider area before dissipating into the fluid. A quantitative estimate of this spreading would be of interest to precisely determine the fluid side wall temperature and heat transfer coefficient. However, it is not simple to calculate because of the conjugate nature of the problem. In addition, the discrete nature of the MCT heat dissipation on the test section makes it more difficult. A separate axisymmetric case of the same system with uniform circular-ring shaped heat-addition problem was numerically solved using the Phoenics computational fluid dynamics code.[13] Axial variations of the radial wall-heat flux at the inner wall for a typical set of input parameters for both venturi and circular pipe flows are plotted in Fig. 9. The wall thickness and the venturi throat length where heat addition takes place are 3.18 and 2.64 mm, respectively. Heat flux, *Re*, and coolant inlet temperature are shown in the figure. Axial lengths of heat spreading are obtained from the bell-shaped curves (Fig. 9) as the effective lengths across which 90% of the radial heat flow to the coolant takes place. Accordingly, it is determined that the heat addition length of 2.64 mm spreads to 40 mm for the venturi flow case and to 80 mm for the pipe flow case, with both cases using copper

Table 1 MCT cooling test results summary[a]

Serial no.	Test parameter	Venturi flow	Circular pipe flow	Commercial heat sink
1	MCT current, A	95.08	75.02	63.45
2	MCT voltage drop, Vdc	1.789	1.551	1.455
3	Applied voltage, Vdc	4.516	3.626	3.253
4	MCT power dissipation, W	170.09	116.33	92.34
5	Applied power, W	429.4	272.0	206.4
6	MCT temperature, °C			
	Top (junction)	168.5	161.1	154.9
	Bottom (case)	132.3	138.0	116.0
	Flange	112.3	118.1	84.6
7	Coolant flow rate, l/min	2.52[b]	5.05[b]	5.05
8	Reynolds number	10,716/5,445[c]	21,432	9,365
9	Coolant temperature, °C	6.5	6.5	6.5
10	Thermal resistance, °C/W			
	Junction-to-case	0.213	0.199	0.421
	Device-to-fluid	0.952	1.329	1.607
11	Heat flux, W/cm^2			
	At internal substrate solder, 0.66 cm^2	257.7	176.3	139.9
	At the base of MCT, 1.8 cm^2	94.5	64.6	51.3
12	Test log			
	Number	V30	C22	W10
	Date	10/15/92	10/13/92	10/29/92

[a]Peak performance data compared for three cooling configurations.
[b]One-sixth of total flow rate.
[c]Reynolds number, upstream/downstream of throat.

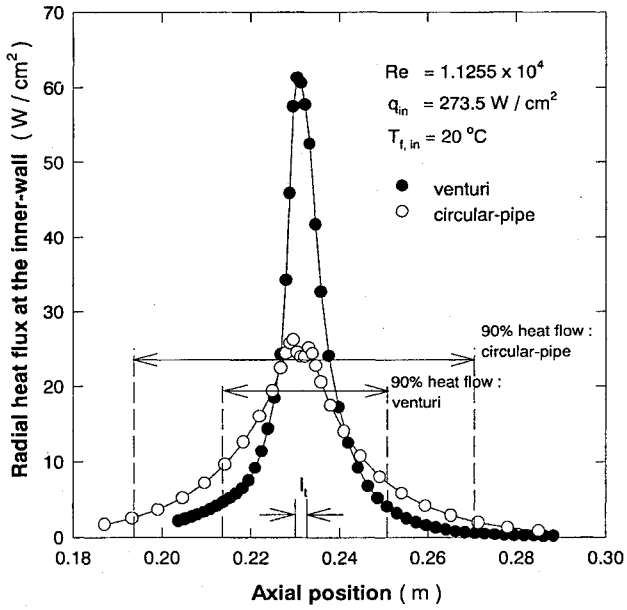

Fig. 9 Illustration of heat-spreading in the wall at the throat.

as the wall material and water as the coolant. A detailed description of this can be found in Ref. 13.

Peak Performance Results Summary

The peak performance was judged from the largest MCT current handled in the conduction mode testing for any heat sink tested without exceeding the safe operating temperature for the MCT. Table 1 provides this comparison at a coolant temperature of 6.5°C as a common reference for the three cases. The coolant flow rates given for the venturi and pipe flows are one-sixth of the total flow. Here, it is assumed that the cooling effect of the flow is equally shared between the six faces of the hexagonal geometry. Venturi flow case exhibited the largest MCT current of 95 A, which was very close to the rated value of 100 A. Also listed in this table are thermal resistances and heat flux values.

Thermal resistance:

$$\text{junction-to-case,}\quad \theta_{JC} = (T_{Top} - T_{Bottom})/P_{MCT}$$

$$\text{device-to-fluid,}\quad \theta_{DF} = (T_{Top} - T_{Fluid})/P_{MCT}$$

Heat flux:

$$\text{at internal substrate solder,}\quad q_1 = P_{MCT}/A_{Substrate}$$

$$\text{at the base of MCT,}\quad q_2 = P_{MCT}/A_{Base}$$

where T is measured MCT temperature and P is MCT power that is the product of measured circuit current and forward voltage drop. The substrate and base area of the MO-93 package were 0.66 and 1.8 cm^2, respectively.

Temperature vs Coolant Flow

At a moderate circuit current of 60 A, MCT top surface temperatures were compared for all three cases as a function of flow rate. An interesting plot resulted, as shown in Fig. 10, where the temperature values were the highest for the commercial heat sink and the lowest for the venturi flow. Temperature dropped initially and steadied as flow rate increased for configurations II and III, whereas that for venturi flow exhibited a steep drop beyond 4 l/min. The steep drop in MCT temperature for high flow rates in the case of venturi flow is explained as follows. If the MCT temperature is high enough to cause the fluid side wall temperature to raise above the saturation temperature of water, phase change could be occurring locally at the heat transfer site. A thin layer of vapor film or blanket here would certainly reduce heat transfer. It is evident from the figure that for the one-sixth flow rate < 4 l/min ($Re < 1.6 \times 10^4$) all of the flow configurations operated at this transition regime of water (100°C) as the ΔT between MCT top surface and inner wall is approximately 20–40°C. At higher flow rates ($Re > 1.6 \times 10^4$), flow velocity at the throat is sufficient enough to clear the vapor film and bring the heat transfer to single phase for the venturi flow only. This exemplifies the distinct advantage of the venturi cooling concept. Figure 11 shows the temperature variation and θ_{DF} for all three cases as functions of coolant temperature for a constant flow rate. Venturi flow exhibited better performance at lower T_{Fluid}.

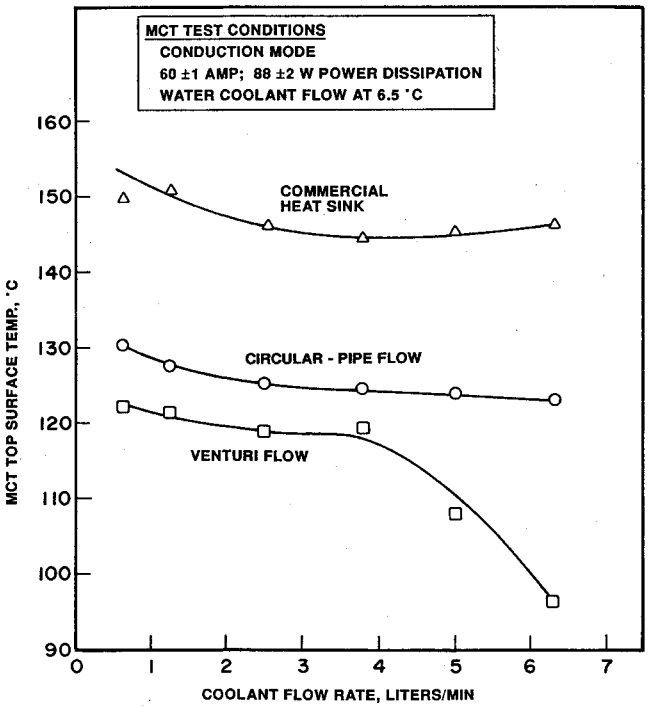

Fig. 10 MCT top-surface temperature vs coolant flow rate.

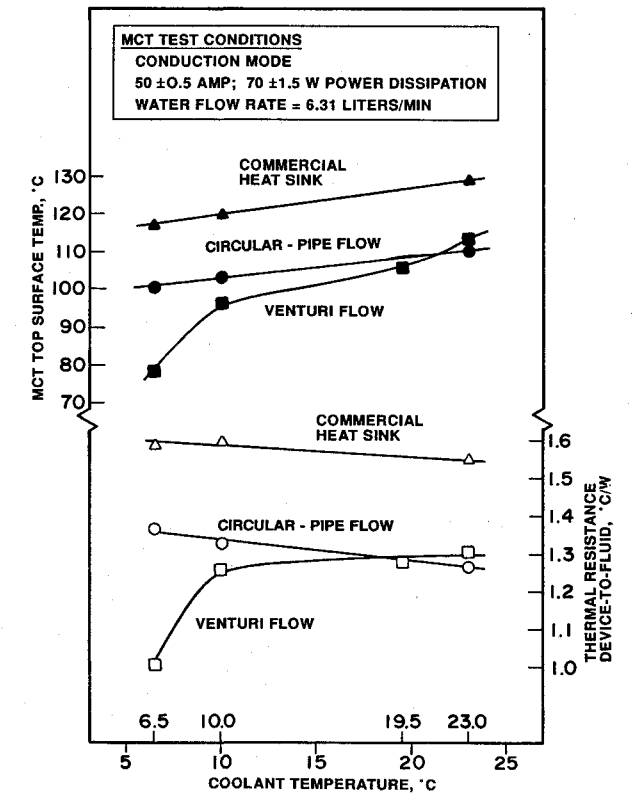

Fig. 11 MCT top-surface temperature and thermal resistance (θ_{DF}).

Thermal Resistance vs MCT Power

θ_{JC} and θ_{DF} were plotted as functions of MCT power for all three cases at T_{Fluid} = 6.5°C and a flow rate of 2.52 l/min as seen in Fig. 12. θ_{DF} values were larger than θ_{JC} for all cases as θ_{DF} includes the external thermal resistances such as contact resistance, wall conduction, and wall-to-fluid resistance. θ_{JC} includes only the internal MCT substrate bonding resistances and body (casing) resistance. In the case of commercial heat

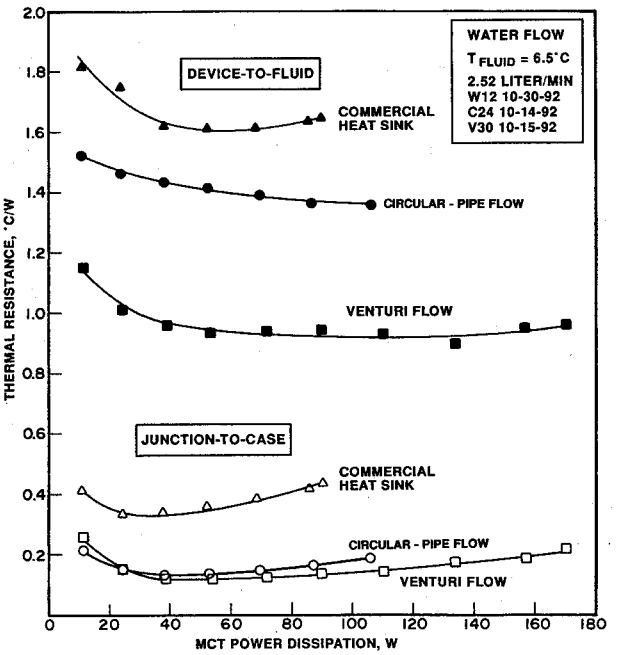

Fig. 12 Thermal resistance vs power dissipation.

sink test, θ_{JC} was higher than that for the other two configurations. The reasons may be attributed to higher MCT operating temperature and nonuniform cooling of the MCT bottom by the commercial heat sink. Also, with high operating temperature, the substrate bonds could weaken and exhibit high thermal resistance. This discrepancy was not observed for circular and venturi flows wherein θ_{JC} values were more or less equal.

The θ_{DF} values of the MCT in Fig. 12 clearly demonstrate again that venturi flow is superior to the other cases. The decrease in θ_{DF} up to an MCT power of 70 W could be explained by the facts that the internal MCT substrate bonding and packaging materials expand with heating and their thermal conductivities vary with temperature.

Conclusions

Single-phase liquid cooling of an MCT device using an annular venturi-type flow was successfully demonstrated. This cooling method has proved very effective for localized high heat flux applications. A comparison of performance results between commercial liquid-cooled cold plate, pipe flow, and venturi flow heat sinks showed superior performance by the venturi flow. Coolant flow rate increase and coolant temperature decrease produced a sharp drop in device temperature and device-to-fluid thermal resistance, respectively, for the venturi flow and was not seen for pipe flows. The venturi flow cooling technique is suitable for any localized high heat flux applications such as the MCT cooling. Use of other coolants and geometry optimization are possible. The liquid pressure drop penalty due to venturi constriction is only marginal.

Acknowledgments

This work was funded by the Aero Propulsion and Power Directorate of Wright Laboratory through U.S. Air Force Contract F33615-91-C-2104 and was supported by the in-house research facilities of the Power Technology Branch's Thermal Laboratory and Power Components Branch's Electrical Technology Laboratory. The authors thank V. Shanmugasundaram for providing the computational analysis results. Technical assistances provided by J. Tennant, M. Ryan, and D. Reinmuller are acknowledged.

References

[1]Temple, V. A. K., "Mos-Controlled Thyristors—A New Class of Devices," *IEEE Trans Electron Devices*, Vol. ED-33, No. 10, 1986, pp. 1609–1618.

[2]Radun, A., and Richter, E., "A Detailed Power Inverter Design for a 250 kW Switched Reluctance Aircraft Engine Starter/Generator," Society of Automotive Engineers Paper 931388, April 1993.

[3]Mackowski, M., "Requirements for High Flux Cooling of Future Avionics Systems," Society of Automotive Engineers Aerospace Technology Conf. and Exposition, SAE Paper 912104, Long Beach, CA, Sept. 1991.

[4]Gu, C. B., Chow, L. C., and Beam, J. E., "Flow Boiling in a Curved Channel," *Heat Transfer in High Energy/High Heat Flux Applications*, American Society of Mechanical Engineers, HTD Vol. 119, 1989.

[5]Iversen, A. H., "Thermal Management of High Flux Electronic Components in Space and Aircraft Systems," Final Rept. by Coriolis Corp., AF Rept. WRDC-TR-90-2122, SBIR Phase I, 1991.

[6]Wadsworth, D. C., and Mudawar, I., "Enhancement of Single-Phases Heat Transfer and CHF from an Ultra-High-Flux Simulated Microelectronic Heat Source to a Rectangular Impinging Jet of Dielectric Liquid," *Advances in Electronic Packaging*, Vol. 1, American Society of Mechanical Engineers, New York, 1992, pp. 143–151.

[7]Ponnappan, R., Reyes, A. S., and Beam, J. E., "Venturi Flow Cooling Concept for High Heat Flux Applications," *Advances in Electronic Packaging*, Vol. 1, American Society of Mechanical Engineers, New York, 1992, pp. 225–234.

[8]Ponnappan, R., and Beam, J. E., "A Novel Electronic Cooling Concept," *Proceedings of the 27th Intersociety Energy Conversion Engineering Conference*, Vol. 2, Aug. 1992, pp. 411–416 (SAE Paper 929478).

[9]Ponnappan, R., Leland, J. E., Chang, W. S., and Beam, J. E., "Results of a Single Phase Venturi Flow," *Proceedings of the 6th International Symposium on Transport Phenomena in Thermal Engineering* (Seoul, Republic of Korea), Vol. 2, 1993, pp. 1225–1231.

[10]Ponnappan, R., and Leland, J. E., "Forced-Convection Heat Transfer in a Venturi-Type Annular Flow," *Proceedings of the 1st ISHMT-ASME Heat and Mass Transfer Conference*, edited by Balakrishnan and Murthy, Tata, McGraw–Hill, New York, 1994, pp. 197–203.

[11]Reyes, A. S., Nguyen, B. T., Weimer, J. A., Beam, J. E., and Chow, L. C., "Operation Characteristics of a MOS Controlled Thyristor (MCT) Using a Liquid Cooling Approach," *Proceedings of the 27th Intersociety Energy Conversion Engineering Conference*, Vol. 2, 1992, pp. 2.405–2.410 (SAE Paper 929477).

[12]*Innovative Thermal Management Solutions—Components for Liquid-Cooled Systems*, EG&G Wakefield Engineering, Active Cooling Products Catalog, Wakefield, MA, 1988.

[13]Shanmugasundaram, V., Ponnappan, R., Leland, J. E., and Beam, J. E., "Conjugate Heat Transfer in Venturi-Type Cooling System: Numerical and Experimental Studies," AIAA Paper 95-2114, June 1995.